Polymer composites

Embedded Carbon-Nanotube-Stiffened Polymer Surfaces**

Nachiket R. Raravikar, Aravind S. Vijayaraghavan, Pawel Keblinski, Linda S. Schadler, and Pulickel M. Ajayan**

Conducting surface coatings are useful for antistatic applications,[1] whereas surface hardening of materials is useful for improving the wear and abrasion resistance.[2,3] For polymer materials, surface conductivity and stiffness may be improved by applying coatings or adding fillers to the polymer matrix.[1,4] For example, polymers can be made scratch resistant by the addition of hard fillers.[4] However, for the case of polymers, achieving excellent mechanical and electrical properties only at the surface is a challenge. Conventional hard fillers, such as alumina or silica, improve the scratch resistance of the polymer,[4] but do not help improve the conductivity. On the other hand, conducting fillers such as micrometer-scale graphite particles[1] do not considerably improve the mechanical properties of the polymer. Thus, there is a need to develop a surface engineering approach to alter the mechanical and electrical properties of polymer coatings.

Multiwalled carbon nanotubes (MWNTs) are stiff macromolecular structures having outer diameters of $\approx$30 nm, and lengths on the order of a few tens of micrometers.[5] The MWNTs also have a very high conductivity ($\approx 10^5$ S cm^{-1}),[6] high modulus ($\approx$1 TPa) along their length direction,[5] as well as a high bending modulus (0.9 to 1.24 TPa).[7] Possibilities of improving bulk mechanical and electrical properties of composites by nanotube-reinforcement have been discussed in the literature.[1,6,8–12] For example, the polymer-intercalated nanotube sheets have shown significant improvement in the modulus of the film.[12] Our approach is to incorporate the excellent properties of nanotubes at a polymer surface in a well-ordered and distributed fashion resulting in the improvement in the electrical as well as mechanical properties of the polymer. This would enable multifunctional surface characteristics for polymer coatings. This paper describes the first report of the generation of such surface-engineered polymer coatings with nanotubes.

In the present work, a thickness-aligned MWNT/polymer disc was prepared, where the MWNTs were reinforced into one of the surfaces of the disc, and were aligned in the thickness direction. The discs were made from two different polymers: polymethyl methacrylate (PMMA) and polydimethyl siloxane (PDMS).[13,14] Both PMMA and PDMS are insulating. However, PMMA is a glassy, rigid polymer at room temperature, whereas PDMS is a soft elastomer at room temperature. The synthesis of the composite disc was performed as follows:[14] First, the aligned arrays of MWNTs ($\approx$30 μm in length) were grown on a quartz substrate by chemical vapor deposition.[14,15] Subsequently, the quartz substrate with aligned nanotube arrays was gently immersed, with the nanotube side facing the top, into the excess monomer (or uncured resin) solution in a vial. By using the excess quantity, the resulting polymer not only occupied the inter-nanotube gaps in the MWNT arrays, but also formed a thick layer above the surface of the MWNT arrays. A portion of the same monomer solution was taken in a separate vial to make pure polymer as a control sample. After the in situ polymerization was complete, polymer discs were taken out of the quartz substrate. In order to make MWNT/PMMA discs, the monomer (methyl methacrylate (MMA)), the initiator (2,2′-azobisisobutyronitrile (AIBN)), and the chain-transfer agent (1-decanethiol) were mixed together in a given proportion (60 mL MMA: 0.17 g AIBN: 30 μL 1-decanethiol) in a quartz vial.[14,16] The polymerization was carried out in a water bath at 55 °C, for 24 h. The weight fraction of MWNTs in the MWNT/PMMA composite films was estimated to be approximately 4 %.[14] Schematics of the synthesis process and the cross-sectional SEM micrographs of the thickness-aligned MWNT/PMMA discs are shown in Figure 1. Similarly, PDMS as well as MWNT/PDMS films were prepared by infiltration of a mixture of silane resin and a curing agent (in a proportion of 10:1 by weight) into aligned MWNT arrays, followed by typical thermal cure cycles.

The surface resistivity of the MWNT side of the polymer disc was compared with that of the pure PMMA side by measurement with a four-probe setup with a probe spacing of $\approx$500 μm. A dc current (I), on the order of a few hundred microamps, was applied through the sample, and the voltage (V) was measured in millivolts. The MWNT-reinforced side of the PMMA disc showed a dc conductivity of 0.60 ± 0.07 S cm^{-1}, whereas the pure PMMA side was not conducting. The reported conductivity of PMMA is $\approx 5 \times 10^{-11}$ S cm^{-1}.[6] Thus, the addition of MWNTs increases the surface conductivity of PMMA significantly. The MWNTs used in the present analysis are macroscopically aligned but show less overall alignment owing to the waviness of the nanotubes. Thus, the percolation threshold is expected to be drastically lower than that which is expected for perfectly aligned fibers in a matrix. Therefore, the nanotube loading ($\approx$4 % by weight or 2 % by volume) in the present composites is expected to be above percolation threshold, as indicated by the conductivity of 0.60 ± 0.07 S cm^{-1}. This value is higher than that reported in the literature for similar loadings of pure, non-aligned MWNTs (10^{-3} to 10^{-2} S cm^{-1}),[6,11] but lower than for similar loadings of Fe-containing MWNTs in PMMA (>1 S cm^{-1}).[11] The conductivity of the aligned MWNT/PMMA surfaces is large enough for poten-

[*] Dr. N. R. Raravikar,[+] A. S. Vijayaraghavan,[+] Prof. P. Keblinski, Prof. L. S. Schadler, Prof. P. M. Ajayan
Departments of Materials Science and Engineering
Rensselaer Polytechnic Institute, Troy, NY 12180 (USA)
Fax: (+1) 518-276-8554
E-mail: schadl@rpi.edu
ajayan@rpi.edu

[+] These authors contributed equally to the work

[**] This work was supported through the Nanoscale Science and Engineering Initiative of the National Science Foundation (NSF).

 DOI: 10.1002/smll.200400064

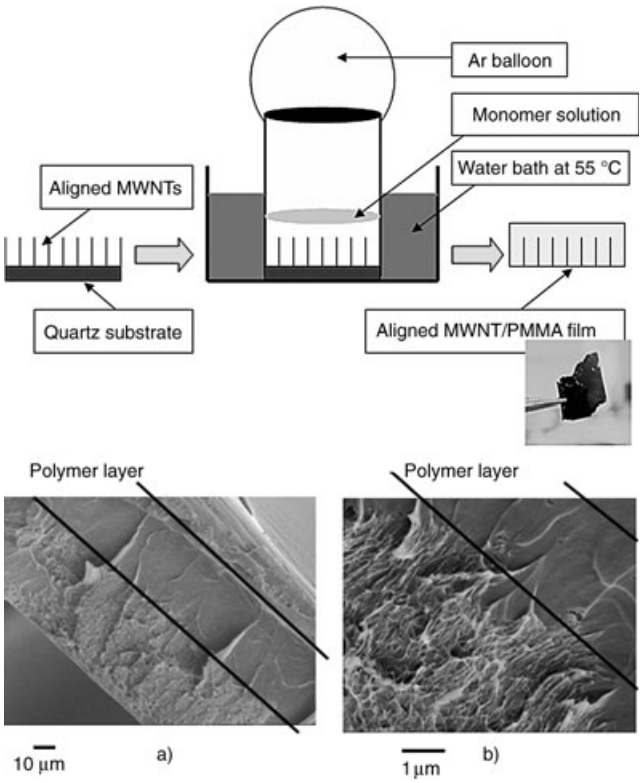

Figure 1. A schematic of the infiltration and in situ polymerization of MMA in aligned MWNT arrays. SEM images of the resulting thickness-aligned MWNT/PMMA films are shown in (a) and (b).

tial antistatic coatings on otherwise insulating polymers.[1,6,8–11]

The surface mechanical properties of the thickness-aligned MWNT/polymer composites were studied using Vicker's microhardness as well as through the force curves generated using atomic force microscopy (AFM). Vicker's microhardness data is shown in Figure 2 and the force curves obtained using AFM are shown in Figure 3. In an AFM experiment, a conical tip having a tip diameter of ≈ 10 nm and a cone-apex angle of $\approx 20°$ was indented into the sample. Force curves were generated by indenting the surface of a composite film as well as that of a pure polymer control sample with an AFM tip, up to the same cantilever deflection (same maximum force). An etched silicon cantilever with a force constant of 60–100 $N\,m^{-1}$ was chosen for indentation by AFM. The cantilever was calibrated before and after indentation on a hard surface to determine its sensitivity. The indentation was carried out at regular intervals on a $2 \times 2\ \mu m^2$ area. The force curves generated were then converted to load-versus-indentation curves, and subsequently used to analyze the local elastic properties of the surface. The effective surface stiffness was used to qualitatively compare the mechanical properties of the pure and

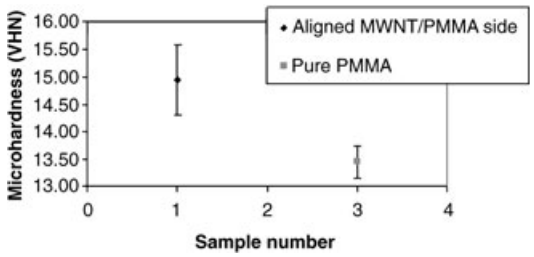

Figure 2. Comparison of Vicker's microhardness of the MWNT-reinforced surface of PMMA with pure PMMA. The Vicker's hardness number,[2] $(VHN) = 2P[\sin(\theta/2)]/L^2 = 1.854P/L^2$, where P is the load (≈ 25 gf), L is the average length of the diagonals obtained by microscopic measurements, and θ is the included angle between diagonals ($\approx 136°$). The VHN was obtained from the standard charts for given P and L, and was averaged over ≈ 15 readings. The MWNT-reinforced surface of PMMA shows $\approx 10\%$ improvement in the microhardness of the polymer.

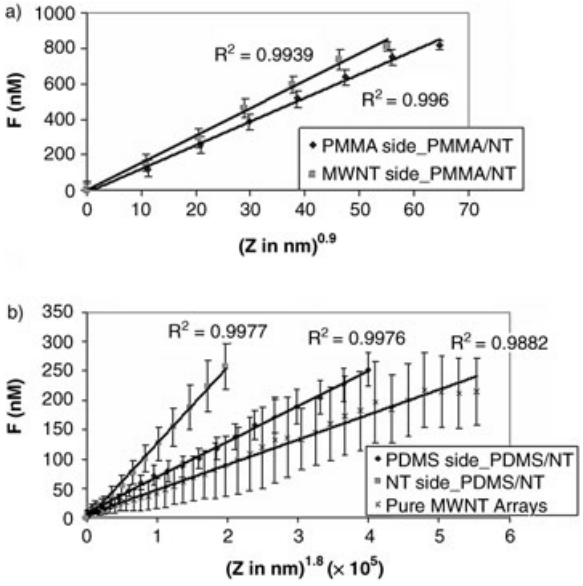

Figure 3. a) The MWNT-reinforced surface of PMMA shows an increase of $\approx 18\%$ in the effective surface stiffness of the polymer; b) the MWNT-reinforced surface of a PDMS film, compared with pure PDMS, shows an improvement of $\approx 140\%$ in the effective surface stiffness of the latter.

Editorial Advisory Board Member

Pulickel Ajayan earned his B Tech in metallurgical engineering from Banaras Hindu University (1985) and PhD in materials science and engineering from Northwestern University (1989). After three years of postdoctoral experience at NEC Corporation in Japan, he spent two years as a research scientist at the Laboratoire de Physique des Solides, Orsay (France) and a year and a half as an Alexander von Humboldt fellow at the Max-Planck-Institut für Metallforschung, Stuttgart (Germany). In 1997, he joined the faculty at Rensselaer and is presently the Henry Burlage Professor of Materials Science and Engineering. His research interests include synthesis and structure–property relations of nanostructures and nanocomposites, applications of nanomaterials, phase stability in nanoscale systems, and electron microscopy. He is one of the pioneers in the field of carbon nanotubes.

MWNT-reinforced polymer surfaces.[17] In order to determine the effective surface stiffness in the present case, only the loading portion of the force curve was used.[17] Very small loads, on the order of a few hundred nN, were used in this test to produce only elastic deformation of the sample surface. The AFM was used in tapping-mode to scan the surface topography before and after the indentation was carried out. There was no apparent change or damage on the surface of the sample. This, in addition to the repeatability of the force curves at the same location over time, indicates that indentation of the tip into the surface produces a purely elastic deformation. The effective surface stiffness was obtained as the slope of the load-versus-indentation curves. Such curves for MWNT/PMMA and MWNT/PDMS surfaces are shown in Figure 3a and b, respectively. It should be noted that the elastic modulus of the sample cannot be obtained directly using the present approach. For estimation of the elastic modulus, the unloading portion of the force curve is typically used and the nano-indentation of the surface involves plastic deformation.[18–19]

A comparison of the Vicker's microhardness data shows $\approx 10\,\%$ improvement in the microhardness of the aligned-MWNT-reinforced PMMA over pure PMMA. A comparison of AFM force curves taken on the MWNT side of the MWNT/PMMA films against pure PMMA indicates that the MWNT-reinforced surface is stiffer than that of pure PMMA. An increase of $\approx 18\,\%$ in the effective surface stiffness of MWNT-reinforced PMMA is observed over that of pure PMMA. Since the microhardness and the effective surface stiffness are both proportional to the elastic modulus of a sample, the results shown by AFM and Vicker's tests are consistent. The surface mechanical properties of the nanotube-reinforced surface of PDMS are also compared with those of the pure PDMS surface. An increase of $\approx 140\,\%$ is observed in the slope of the force curve measured for a MWNT-reinforced surface of PDMS over that of the pure PDMS. The results imply that nanotube-reinforcement results in substantial stiffening of the polymer surfaces.

On an absolute scale, the slope of the MWNT-reinforced PDMS surface is almost three orders of magnitude lower than that of the MWNT-reinforced PMMA surface. This is because the modulus of the pure PDMS matrix is lower than that of PMMA by about the same order of magnitude. A relationship between the observed improvement in the effective surface stiffness and the modulus of the matrix can be obtained by considering the buckling of the wavy fibers reinforced in a composite. Both AFM and Vicker's microhardness tests use compressive loads, which causes bending and buckling of nanotubes under compression. Also, the MWNTs in the present case are wavy and not perfectly straight. It is reported[20–21] that the stiffness and the strength of carbon fibers are drastically reduced due to fiber waviness, as compared to those of the straight fibers. Fiber waviness reduces the resulting modulus of the fiber–polymer composite, to lower than that predicted by the rule of mixtures.[20–22] Piggott[22] and other groups[20–25] have analyzed the compressive strength and modulus of composites in the fiber-axis direction, by assuming the fibers to be wavy (sinusoidal) and embedded in a soft as well as a hard matrix. In their analysis, a soft matrix is defined as a matrix where the Young's modulus, $E_{\text{fiber}} \gg E_{\text{matrix}}$. This analysis can be applied to the present case by assuming a soft matrix, where $E_{\text{MWNT}} \gg E_{\text{PDMS}}$ and E_{PMMA}. The amplitude and wavelength of the fiber (diameter d) are characterized by the dimensionless parameters a and λ, respectively. Straight fibers will decrease in length when compressed,[26] with a compliance of $1/E_{\text{f}}$, where E_{f} is the Young's modulus of the fiber. On the other hand, curved fibers will suffer an increase in amplitude a and decrease in wavelength λ of the curvature as a result of pushing against the matrix at right angles to the fiber alignment direction. This will contribute an additional compliance, $1/E_{\text{fl}}$ (in addition to the original $1/E_{\text{f}}$) which, for long specimens with length greater than λ is given by:[22]

$$E_{\text{fl}} = \lambda^4 E_{\text{m}}/\pi^5 a^3 \tag{1}$$

All other parameters (such as the initial fiber waviness) being constant, $E_{\text{fl}} \alpha E_{\text{m}}$. The waviness-induced fiber compliance, $1/E_{\text{fl}}$, further modifies the rule of mixtures as,[22]

$$E_1 = Vf/(1/E_{\text{f}} + 1/E_{\text{fl}}) + V_{\text{m}} E_{\text{m}} \tag{2}$$

Thus the composite modulus E_1 is a strong function of the matrix modulus E_{m} due to fiber waviness. A schematic of stress distribution around a wavy fiber-reinforced composite is shown in Figure 4a. The normalized effective surface stiffness of the MWNT-reinforced side of a polymer is plotted as a function of the effective surface stiffness of the re-

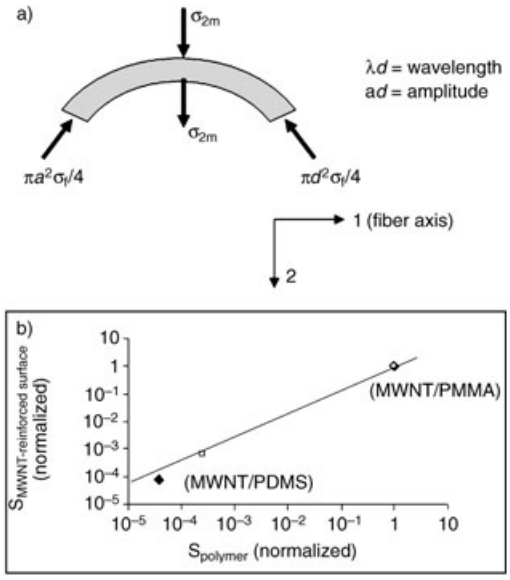

Figure 4. a) Schematic of stress distribution around a wavy fiber reinforced in a polymer matrix. (σ_{2m} is the stress on the matrix, σ_f is the stress on the fiber, d is the diameter of the fiber); b) $S_{\text{MWNT-reinforced surface}}$ (normalized) is the normalized effective surface stiffness of the MWNT-reinforced surface as measured by AFM. S_{polymer} (normalized) is the normalized effective surface stiffness of the polymer as measured by AFM. The solid line is the theoretical proportionality between the composite modulus, E_1(normalized) and matrix modulus E_{m}(normalized). The effective surface stiffness of the nanotube-reinforced surface scales with that of the polymer matrix surrounding the nanotubes.

spective pure polymer, in Figure 4b. Figure 4b shows that the normalized effective stiffness of a nanotube-reinforced surface [$S_{\text{MWNT-reinforced surface}}$ (normalized)] increases with that of the pure polymer [S_{polymer} (normalized)]. The plot has two data points; one for PDMS and the other for PMMA. These data points follow the above-mentioned proportionality, $E_{\text{f1}} \alpha E_{\text{m}}$. According to the above relationship, as E_{m} (or S_{polymer}) approaches zero, E_{f1} (or $S_{\text{MWNT-reinforced surface}}$) should also approach zero. This is indicated by a very low value for S_{MWNT} in air, as observed from Figure 3b.

In conclusion, it has been shown that surface electrical and mechanical properties of the polymer can be engineered by nanotube reinforcements at the surface. The surface conductivity of insulating polymers is improved due to the presence of nanotubes. The nanotube reinforcement causes significant improvement in the microhardness of the polymer under compressive loads. This is explained in terms of improvement in the effective stiffness of the composite surface. The latter is proportional to the stiffness of the surrounding polymer matrix. The stiffer the polymer, the larger the resistance of nanotubes to buckling, and consequently, the composite surface is also stiffer.

Keywords:
carbon nanotubes · composite materials · conductivity · mechanical properties · surfaces

[1] J. Sandler, M. S. P. Shaffer, T. Prasse, W. Bauhofer, K. Schulte, A. H. Windle, *Polymer* **1999**, *40*, 5967 – 5971.
[2] G. E. Dieter in *Mechanical Metallurgy, SI Metric Ed.*, McGraw-Hill, London, **1988**, pp. 227 – 337.
[3] Y. Lakhtin in *Engineering Physical Metallurgy, 4th ed.*, Mir, Moscow, **1971**, pp. 77 – 236.
[4] Q. Chen, L. S. Schadler, R. W. Siegel, G. C. Irvin, Jr., J. Mendel, *Mater. Res. Soc. Symp. Proc.* **2002**, p. 733E, T1.12.1.
[5] P. M. Ajayan, *Chem. Rev.* **1999**, *99*, 1787 – 1800.
[6] C. Stephan, T. P. Nguyen, B. Lahr, W. Blau, S. Lefrant, O. Chauvet, *J. Mater. Res.* **2002**, *17*, 396 – 400.
[7] H. J. Qi, K. B. K. Teo, K. K. S. Lau, M. C. Boyce, W. I. Milne, J. Robertson, K. K. Gleason, *J. Mech. Phys. Solids* **2003**, *51*, 2213 – 2237.
[8] B. Safadi, R. Andrews, E. A. Grulke, *J. Appl. Polym. Sci.* **2002**, *84*, 2660 – 2669.
[9] F. Du, J. E. Fischer, K. I. Winey, *J. Polym. Sci. Part B* **2003**, *41*, 3333 – 3338.
[10] B. Philip, J. K. Abraham, A. Chandrasekar, V. K. Varadan, *Smart Mater. Struct.* **2003**, *12*, 935 – 939.
[11] H. M. Kim, K. Kim, C. Y. Lee, J. Joo, S. J. Cho, H. S. Yoon, D. A. Pejaković, J. W. Yoo, A. J. Epstein, *Appl. Phys. Lett.* **2004**, *84*, 589.
[12] J. N. Coleman, W. J. Blau, A. B. Dalton, E. Muňoz, S. Collins, B. G. Kim, J. Razal, M. Selvidge, G. Vieiro, R. H. Baughman, *Appl. Phys. Lett.* **2003**, *82*, 1682 – 1684.
[13] E. Lahiff, C. Y. Ryu, S. Curran, A. I. Minett, W. J. Blau, P. M. Ajayan, *Nano Lett.* **2003**, *3*, 1333 – 1337.
[14] N. R. Raravikar, PhD thesis, Rensselaer Polytechnic Institute (USA), **2004**.
[15] Z. J. Zhang, B. Q. Wei, G. Ramanath, P. M. Ajayan, *Appl. Phys. Lett.* **2000**, *77*, 3764 – 3766.
[16] S. T. Balke, A. E. Hamielec, *J. Appl. Polym. Sci.* **1973**, *17*, 905.
[17] M. R. Vanlandingham, S. H. McKnight, G. R. Palmese, R. F. Eduljee, J. W. Gillespie, R. L. McCullough, *J. Mater. Sci. Lett.* **1997**, *16*, 117 – 119.
[18] M. R. VanLandingham, S. H. McKnight, G. R. Palmese, X. Huang, T. A. Bogetti, R. F. Eduljee, J. W. Gillespie, Jr., *J. Adhesion* **1997**, *64*, 31.
[19] S. M. Hues, C. F. Draper, R. J. Colton, *J. Vac. Sci. Technol. B* **1994**, *12*, 2211 – 2214.
[20] S. Timoshenko in *Theory of Elastic Stability, 1st ed.*, McGraw-Hill, New York, **1936**.
[21] H. M. Hsiao, I. M. Daniel, *Compos. Sci. Technol.* **1996**, *56*, 581 – 593.
[22] M. R. Piggott, *J. Mater. Sci.* **1981**, *16*, 2837 – 2845.
[23] P. M. Jelf, N. A. Fleck, *J. Compos. Mater.* **1992**, *26*, 2706 – 2720.
[24] N. L. Hancox, *J. Mater. Sci.* **1975**, *10*, 234 – 242.
[25] M. R. Piggott, B. Harris, *J. Mater. Sci.* **1980**, *15*, 2523 – 2538.
[26] O. Lourie, D. M. Cox, H. D. Wagner, *Phys. Rev. Lett.* **1998**, *81*, 1638 – 1641.

Received: August 26, 2004

